THERMOCHEMICAL EVOLUTION OF Sb-Cu ORES AT VENTOSA (BEJA, PORTUGAL)

A. Mateus and J. Figueiras

Dep. Geologia e CREMINER, Faculdade de Ciências da Universidade de Lisboa, Ed. C6, Piso 4, 1749-016 Lisboa

Resumo: A mineralização Sb-Cu de Ventosa é controlada por um dispositivo estrutural complexo, envolvendo cisalhamentos WNW-ESE com forte pendor para SW e uma zona de falha tardia subvertical N-S. Os filões, preferencialmente enquadrados por anfibolitos silicificados, são constituídos por um precipitado hidrotermal polifásico de quartzo-carbonato que contém agregados aleatoriamente distribuídos de sulfuretos e sulfossais; principalmente antimonite, tetraedrite, pirite, arsenopirite e bertierite, a que se associam quantidades menores de calcopirite, marcassite, gudmundite, famatinite, aurostibite, calcostibite, calcocite e covelite. Óxidos mal cristalizados de Sb e/ou Fe-Sb, kermesite e hematite/goethite representam os principais produtos de meteorização. As relações texturais indicam frequentemente a preservação de diversas fases meta-estáveis originadas em diferentes estádios de um percurso evolutivo em arrefecimento entre *ca.* 330ºC e 250ºC e/ou sujeito a variações apreciáveis de fS_2 e fO_2, permitindo discutir alguns aspectos pobremente documentados para o sistema Fe-Cu-Sb-S-As-H-O.

Abstract: The Ventosa Sb-Cu mineralisation is controlled by a complex structural configuration, including WNW-ESE shears with strong SW dip and a late sub-vertical N-S fault zone. The lodes, mainly hosted in silicified amphibolites, comprise a multistage quartz-carbonate hydrothermal precipitate that contains randomly distributed aggregates of sulphides and sulphosalts; mainly stibnite, tetrahedrite, pyrite, arsenopyrite and berthierite, complemented by minor amounts of chalcopyrite, marcasite, gudmundite, famatinite, aurostibite, chalcostibite, chalcocite and covellite. Poorly crystallized Sb and/or Fe-Sb oxides, kermesite and hematite/goethite, are the main products of ore weathering. Textural relationships indicate the preservation of several metastable phases originated at different stages of a cooling path ranging from *ca.* 330ºC to 250ºC and/or subjected to significant changes in fS_2 e fO_2. This allows discussing some poorly documented features for the system Fe-Cu-Sb-S-As-H-O.

1. Introduction

Phase relationships of the systems describing the chemical composition of metal concentrations containing Sb are not completely understood, not only because of the considerable number of components and phases involved, but also because of the fact that at the low temperatures at which many antimony concentrations develop, the chemical reactions in the system are far too sluggish to allow easy equilibration at the laboratory time scales. In the Ventosa prospect (Beja, Portugal), the Sb-Cu ores preserve textural relationships between mineral phases apparently recording quenched non-equilibrium conditions, and their detailed examination may shed some light on several problems remaining in the system Fe-Cu-Sb-S-As-H-O. Therefore both the textural relationships and the compositional variability of some minerals will be used to suggest alternative chemical reactions in the above-mentioned system and also to establish the main physical-chemical constraints to ore deposition.

The prospect is located some 4.5 km SE of Beja, near the southeastern border of the Ventosa-Senhora das Neves-São Brissos structure. The mineralisation is controlled by a complex structural configuration, including WNW-ESE shears with strong SW dip and a late sub-vertical N-S fault zone. The main lodes are hosted in strong silicified amphibolites that can show pyrite dissemination.

2. Data summary

Quartz and carbonates (siderite ± calcite) are the main gangue minerals in the Ventosa lodes, commonly with accessory Fe-chlorite. Quartz aggregates form different generations that display a fairly complete record of the deformational and thermal history of the lodes. Much of this history is prior to the main events of sulphide and sulphosalt deposition, since spatial and textural relationships demonstrate that these minerals only coexist with the late, un-deformed or slightly fractured, quartz generations.

Various stages of sulphide-sulphosalt deposition, separated by fracturing events, can be identified. Fractured masses of tetrahedrite + chalcopyrite + pyrite + berthierite ± stibnite, often poorly preserved, represent the first mineral association. Two different tetrahedrite generations can be recognised in this textural context. Tetrahedrite I occurs as millimetric subeuhedral-anhedral crystals displaying more or less evident intra-granular fractures mainly sealed by polybasite, and rarely by other Sb-Ag sulphosalts (like stephanite and pyrargyrite). Some of these tetrahedrite crystals have thin famatinite fringes, which may in some cases include late and euhedral micrometric arsenopirite crystals. Tetrahedrite II occurs as unfractured bladed crystals commonly pitted and finely inter-grown with arsenopyrite, filling the fracture network of the earlier ore minerals (pyrite, in particular). These late tetrahedrite crystals can be easily distinguished on the basis of their significantly lower zinc content.

Thick chalcostibite and famatinite fringes record the relative instability of tetrahedrite in the final mineralising steps and commonly surround the late aggregates of tetrahedrite. Rare micrometric crystals of aurostibite are also present along the sharp boundaries between tetrahedrite and famatinite. Chalcostibite (± covellite) is interpreted to represent the end product of this late re-equilibrium, since in advanced stages of tetrahedrite decomposition famatinite is no longer recognised. These fringes, especially when optically similar to famatinite, have frequently intermediate compositions between ideal famatinite, tetrahedrite and chalcostibite. This suggests that the reactions involved in tetrahedrite decomposition and the formation of the new mineral phases proceeded along a very irregular front or by means of multiple nucleation.

The most important Sb-bearing assemblage, comprising stibnite and iron sulphides, postdates the mineral association described above and grew in part at its expense. Stibnite is the main mineral and generally forms centimetric crystals scattered within late quartz aggregates. In many cases, however, stibnite is associated with pyrite-marcasite intergrowths, whose development is ascribable to berthierite alteration, since this mineral is always present as relic. In some of these intergrowths, particularly along the irregular boundaries of berthierite relics, micrometric crystals of gudmundite can be recognised, suggesting that this sulphide is an intermediate phase in the chemical path of berthierite decomposition.

Arsenopyrite deposition is restricted to the latest mineralising stages. It forms two distinct generations, the last one comprising un-deformed and randomly distributed euhedral crystals or tiny irregular blades inter-grown with late tetrahedrite and/or pyrite aggregates. Chemically, arsenopyrite crystals are slightly As deficient, although, at least for its first generation, no other As-bearing mineral was crystallising at the same time. Arsenic deficiencies are in most cases compensated by excess sulphur; whenever this is not the case, clearly detectable trace amounts of gold and silver are present, probably due to surface processes like those discussed in Wu & Delbove (1989) and Wu *et al.* (1990).

Apart from an earlier, very fractured generation of pyrite, this sulphide displays a very good record of the transition between the main Sb-Cu event and the immediately subsequent Sb event. In fact, the second generation of pyrite is in textural equilibrium with tetrahedrite and includes micrometric grains of chalcopyrite, whereas the third generation is a by-product of berthierite decomposition. Despite the large textural diversity, pyrite is almost stoichiometric, recording just a very slight As-increase in the latest generation, which co-precipitated with arsenopyrite.

Supergene minerals include poorly crystallized Sb and/or Fe-Sb oxides (tentatively identified as schafarzikite - $FeSb_2O_2$ - and tripuhyite - $FeSbO_4$) and hematite and goethite, which in some cases contain fine aggregates of kermesite and covellite-chalcocite.

4. Thermochemical evolution of the Sb-Cu ores; discussion

A physical-chemical interpretation of the paragenesis and textures observed at Ventosa needs a thorough understanding of the system Fe-Cu-Sb-S-As-H-O. However, to our knowledge, only parts of this system have been investigated so far. Therefore, a tentative interpretation of the mineral assemblages of Ventosa will have to rely on results such as those obtained by Williams-Jones & Normand (1997) for the Fe-Sb-S-O subsystem and by Seal *et al.* (1992) for the Cu-Fe-As-S and Cu-Fe-Sb-S subsystems. Note, however, that the juxtaposition of these three subsystems will lead at most to a limited insight in the total system Fe-Cu-Sb-S-As-H-O, because large uncertainties exist in the temperature of some of the invariant points and because of inaccurate experimental data for the low temperature regions of those subsystems caused by the presence of high kinetic barriers or by very sluggish

reaction rates. Nevertheless, if such juxtaposition is used, some diagrams can be drawn (Figs. 1 and 2), to help interpret the observed mineralogical/textural record.

As mentioned above, the earliest mineral association is represented by fractured masses of tetrahedrite, chalcopyrite, pyrite, berthierite and, occasionally, stibnite. The absence of arsenopyrite and pyrrhotite suggests temperatures lower than ≈330ºC and fS_2 values not very far from 10^{-9}, provided that the lack of arsenopyrite is not due to the absence of arsenic in the system; if this was the case, then this earliest association can not be so well constrained in terms of temperature and fS_2. On the other hand, if 300ºC is assumed as a good temperature estimate, the coexistence of tetrahedrite and siderite seems to confirm the fS_2 value and to fix fO_2 at about 10^{-32}.

Fig. 1: Some reaction lines of the system Cu-Fe-Sb-(As)-S as a function of T and fS_2. Thermodynamic data from Seal *et al.* (1990, 1992), Williams-Jones & Normand (1997) and references therein; Aspy-limiting reactions are plotted just for reference. As^0 - native arsenic; Aspy - arsenopyrite; Bn - Bornite; Brt - Berthierite; Cpy - chalcopyrite; Gud - gudmundite; Lo - löllingite; Po - pyrrhotite; Py – Pyrite; Sb^0 - native antimony; Snj - seinäjokite; Stb - stibnite; Td - Fe-tetrahedrite. The shaded area represents the uncertainty in the fS_2-T estimation for the equilibrium of the earliest ore mineral assemblage.

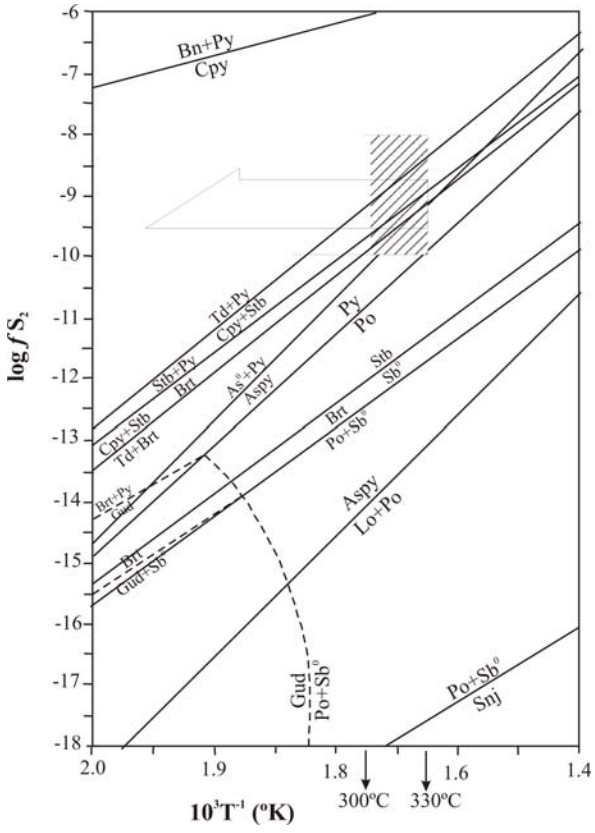

The paragenetic sequence strongly suggests a history of decreasing temperature, as shown by the late occurrence of stibnite and pyrite, together with the absence of pyrrhotite and of stable berthierite. In fact, although berthierite and stibnite occur at the same stage, the former invariably precedes the latter. This may be simply explained by the reaction $FeSb_2S_4 + ½S_2 \Leftrightarrow FeS_2 + Sb_2S_3$ which limits the stability field of berthierite for low temperatures and/or high fS_2. However, the presence of tetrahedrite further complicates the situation because, as temperature decreases and/or fS_2 increases, this mineral will react with berthierite forming stibnite and chalcopyrite: $Cu_{10}Fe_2Sb_4S_{13} + 2FeSb_2S_4 + ½S_2 \Leftrightarrow 10CuFeS_2 + 4Sb_2S_3$. Further temperature decrease or fS_2 increase lead to a reconstitution of tetrahedrite at the expense of both stibnite and chalcopyrite: $10CuFeS_2 + 2Sb_2S_3 + 3/2S_2 \Leftrightarrow Cu_{10}Fe_2Sb_4S_{13} + 8FeS_2$. It should be noted that, since tetrahedrite composition is not fixed, the lines representing the two reactions above cannot have a fixed position, which may lead to the vanishing of the stability field of chalcopyrite + stibnite, as pointed out by Seal *et al.* (1990).

It can thus be seen that the earliest mineral assemblage does record, not bulk equilibrium conditions, but a sequence of successive stages of re-equilibration of an original paragenesis composed of berthierite and tetrahedrite as the temperature and/or fS_2 changed. Further evidence for the non-equilibrium conditions comes from the occurrence of gudmundite surrounding relics of berthierite. If gudmundite were formed inside its stability field, it would then record temperatures below 280ºC and fS_2 much lower than the values indicated by the remaining minerals present. In fact, gudmundite normally accompanies pyrrhotite and, according to Seal *et al.* (1992) and Williams-Jones & Normand (1997), its stability field is limited by the reactions: $(1-x)FeSbS + x/2S_2 \Leftrightarrow Fe_{1-x}S + (1-x)Sb$; $FeSbS + Sb \Leftrightarrow FeSb_2 + ½S_2$ and $(4-4x)FeSbS \Leftrightarrow (2-2x)FeSb_2 + 2Fe_{1-x}S + (1-2x)S_2$, whose positioning in fig. 1 is difficult because of large uncertainties on the thermal dependence of gudmundite Gibbs free energy. However, these reactions, associating gudmundite to either pyrrhotite or Sb^0, clearly demonstrate that gudmundite cannot be in equilibrium with stibnite, chalcopyrite or pyrite, nor can it record an event in the equilibrium evolutionary path leading from an original paragenesis composed of berthierite and tetrahedrite

to paragenesis including the simple iron, copper and antimony sulphides just mentioned. We are thus lead to the conclusion that, if the gudmundite stability field is not to be much larger than currently thought, gudmundite is a transient product of berthierite breakdown, whose formation may be written as $7FeSb_2S_4 + S_2 \Leftrightarrow 6Sb_2S_3 + 2FeSbS + 5FeS_2$, and whose further degradation may be expressed as $2FeSbS + 5/2\ S_2 \Leftrightarrow 2FeS_2 + Sb_2S_3$, thus reconstructing the reaction $7FeSb_2S_4 + 7/2\ S_2 \Leftrightarrow 7FeS_2 + 7Sb_2S_3$. The association arsenopyrite + As-Fe enriched tetrahedrite ± carbonates essentially characterise late mineralising events, whose equilibrium denotes values of $\log fS_2$ and $\log fO_2$ near -13 and -38, respectively, if 250ºC is assumed as a reasonable estimate for the new temperature conditions. To our knowledge, there are no theoretical or experimental data on the low temperature decomposition of tetrahedrite. However, in the case of Ventosa, textural relationships clearly show that tetrahedrite has decomposed first to famatinite and then to chalcostibite and that famatinite itself ultimately transformed to chalcostibite. In the absence of thermodynamic data for famatinite and chalcostibite, the above textures cannot be interpreted in terms of either a quenched non-equilibrium situation or a record of a continuous path through the stability fields of the minerals involved. In any case, the chemical reactions that took place may be written as $Cu_{10}Fe_2Sb_4S_{13} + 2H_2O + ½S_2 + 2CO_2 \Rightarrow 3Cu_3SbS_4 + CuSbS_2 + 2FeCO_{3(aq)} + 2H_2$ and $Cu_3SbS_4 \Rightarrow CuSbS_2 + 2CuS$, suggesting that CO_2 must be an important component of the last hydrothermal fluid flows (which is compatible with the relative abundance of late un-deformed carbonates).

Fig. 2: Some reaction lines of the systems Cu-Fe-Sb-S (A) and Cu-Fe-As-S (B) as a function of $fS2$ and $fO2$ at 300ºC and 250ºC, respectively. Thermodynamic data from Seal *et al.* (1990, 1992) and references therein. Siderite replaces magnetite above a fixed, but unspecified fCO_2. Abbreviations as in fig. 1; Hem - hematite; Sd - siderite; Tn - Fe-tennantite. Shaded areas represent the stability of mineral assemblages that characterize the earlier (diagram A) and the late (diagram B) steps of the first mineralising event at Ventosa. See text for discussion of the stability of chalcopyrite + stibnite in the presence of tetrahedrite solid solution. Equilibria involving chalcostibite, famatinite, kermesite and other possible mineral phases have been omitted for simplicity and/or because of inaccurate thermodynamic data.

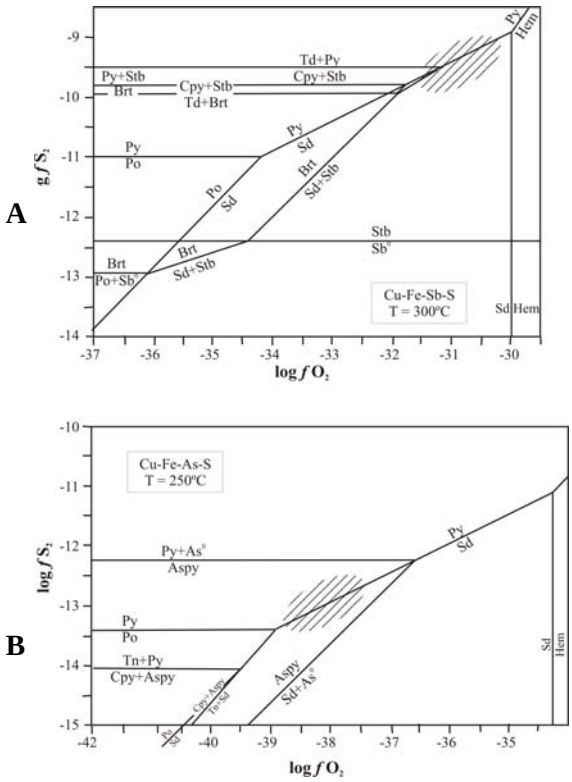

Acknowledgments: MIZOMOR Project (PBICT/P/CTA/2112/95) supported the research.

References

Seal, R.R. II, Essen, E.J., Kelly, W.C., 1990. Tetrahedrite and tennantite: evaluation of thermodynamic data and phase equilibria. Can. Mineral. 28, 725-738.

Seal, R.R. II, Robie, R.A., Barton, P.B. Jr., Hemingway, B., 1992. Superambient heat capacities of synthetic stibnite, berthierite, and chalcostibite: revised thermodynamic properties and implications for phase equilibria. Econ. Geol. 87, 1911-1918.

Williams-Jones, A.E., Normand, C., 1997. Controls of mineral paragenesis in the system Fe-Sb-S-O. Econ. Geol. 92, 308-324.

Wu, X., Delbove, F., 1989. Hydrothermal synthesis of gold-bearing arsenopyrite. Econ. Geol. 84, 2029-2032.

Wu, X., Delbove, F., Touray, J.C., 1990. Conditions of formation of gold-bearing arsenopyrite: a comparison of synthetic crystals with samples from Le Châtelet fold deposit, Creuse, France. Mineral. Deposita 25, S8-S12.